ECOHYDROLOGY
Ecohydrol. **2**, 115–128 (2009)
Published online 24 February 2009 in Wiley InterScience
(www.interscience.wiley.com) DOI: 10.1002/eco.45

'Quantifying the effects of forest canopy cover on net snow accumulation at a continental, mid-latitude site'

W. Veatch,[1]* P. D. Brooks,[1] J. R. Gustafson[1] and N. P. Molotch[2]

[1] *SAHRA and Department of Hydrology and Water Resources, University of Arizona, Tucson, AZ, 85721, USA*
[2] *Department of Civil and Environmental Engineering, University of California, Los Angeles, CA, 90095, USA*

ABSTRACT

Although many studies have investigated the effects of forest cover on streamflow and runoff, and several have examined the effects of canopy density on snowpack accumulation, the impacts of forest canopy density on spatial patterns of snowmelt input to catchments remain relatively underquantified. We performed an intensive snow depth and density survey during maximum accumulation in a mid-latitude montane environment in northern New Mexico, taking 900 snow depth measurements and excavating six snow pits across a continuum of canopy densities. Snow water equivalent (SWE) data are correlated with forest canopy density ($R^2 = 0{\cdot}21,\ p < 0{\cdot}0001$), with maximum snow accumulation in forests with density between 25 and 40%. Forest edges are shown to be highly influential on patterns of snow depth, with unforested areas shaded by forest to their immediate south holding approximately 25% deeper snow than either large open areas or densely forested areas. This indicates that the combination of canopy influences on throughfall and snowpack shading are key processes underlying snow distribution in the high solar load environments typical of mountainous, mid-latitude areas. We further show that statistical models of snow distribution are improved with the addition of remotely sensed forest canopy information (R^2 increased in 10 of 11 cases, deviance lowered in 9 of 11 cases), making these findings broadly relevant for improving estimation of water resources, predicting the ecohydrological implications of vegetation and climate change, and informing integrated forest and water resources management. Copyright © 2009 John Wiley & Sons, Ltd.

KEY WORDS snow accumulation; forest–snow interactions; binary regression tree model; spatial distribution; forest density

Received 28 May 2008; Accepted 1 December 2008

INTRODUCTION

More than 60 million people in the western United States rely on water from mountain river basins for their drinking, irrigation and industrial needs, while more than one billion people globally depend on water from seasonally snow-covered catchments and glaciers (Bales *et al*., 2006). The quantity of water available from these snow-fed rivers, reservoirs and aquifers varies with trends in precipitation and temperature (e.g. Barnett *et al*., 2005) as well as with changes in forest properties (e.g. Ffolliott *et al*., 1989). Recent changes in forest structure and composition have occurred in days to months due to forest fires and outbreaks of insect pests such as pine beetles (Breshears *et al*., 2005), while longer-term shifts in plant species composition have occurred with changes in climate (Webb and Bartlein, 1992) and are expected to continue with future global climate change (Iverson and Prasad, 1998). The combination of these vegetation changes, along with the patterns of disturbance and succession that occur constantly in mountain forests (Day, 1972), hold consequences for water resources that are still poorly understood.

The influence of vegetation properties on spatial patterns of snow depth and water equivalent has long been recognized. Forest cover intercepts precipitation, reducing subcanopy snowfall (Harding and Pomeroy, 1996; Hardy *et al*., 1997; Hedstrom and Pomeroy, 1998; Pomeroy *et al*., 1998b, 2002; Gelfan *et al*., 2004; Musselman *et al*., 2008); influences the net energy available to the snowpack for sublimation and melt by reducing shortwave and increasing longwave radiation (Barry *et al*., 1990; Yamazaki and Kondo, 1992; Hardy *et al*., 1997; Zhang *et al*., 2004; Bales *et al*., 2006; Rinehart *et al*., 2008); and decreases wind speeds, reducing wind redistribution and energy input to the snowpack through reduced turbulent heat exchange (Barry *et al*., 1990; Yamazaki and Kondo, 1992; Wigmosta *et al*., 1994; Harding and Pomeroy, 1996; Hardy *et al*., 1997; Pomeroy *et al*., 1998a; Gelfan *et al*., 2004). These processes result in distinct energy and interception regimes that are reflected in spatial statistical modelling of snow cover (Balk and Elder, 2000; Erxleben *et al*., 2002; Geddes *et al*., 2005), as well as the common observation that small canopy openings frequently hold more snow than either open areas or deep forests (Kuz'min, 1960, cited in Golding and Swanson, 1978; Gelfan *et al*., 2004). Recent studies have shown that sublimation losses from intercepted snowfall and the subcanopy snowpack may remove a large fraction of annual precipitation (Hedstrom and Pomeroy, 1998; Essery *et al*., 2003; Molotch *et al*., 2007), but better knowledge of the spatial distribution of snow and snowmelt is needed before these findings

* Correspondence to: W. Veatch, US Army Corps of Engineers New Orleans District, ED-H, 7400 Leake Ave., New Orleans, LA 70118, USA.
E-mail: William.C.Veatch@usace.army.mil

can be fully utilized to understand hydrological partitioning and ecological function in seasonally snow-covered, forested environments.

Despite increasing knowledge of the effects of forest properties on snow accumulation processes and of the effects of vegetation change on streamflow, relatively little is known about the importance of forest density and structure on water input to the catchment. In particular, the knowledge that small forest openings hold deeper snow is of little help to science and management unless the prevalence and effects of these openings can be quantified at the basin scale, for example through the use of remotely sensed vegetation data. In addition to improving estimates of the spatial distribution of water equivalent, better understanding of the processes linking forests and snow are needed to predict the effects of climate and vegetation change and to quantify the potential benefits of integrated forest and water resources management.

In this study, we evaluated the effects of vegetation density and geometry on maximum snowpack accumulation, and thus springtime snowmelt input to the catchment. Previous work on micro-scale variations in snow water equivalent (SWE)(Musselman *et al*., 2008) implied that the combination of two vegetation-mediated processes, snowfall interception and snowpack shading, would result in maximum snowpack accumulation in forests with moderate density as opposed to either open areas or very dense forest, a hypothesis we test in this paper with an intensive forest stand-scale snow depth and density survey. Secondary objectives of this study included investigating the underlying processes controlling snow accumulation patterns at the stand scale, for which we use a simple model of energy and throughfall regimes in forests and investigating methods of utilizing remotely sensed forest canopy density information to improve statistical models of spatial snow distribution.

STUDY AREA

The study area lies within the 89 000 acre Valles Caldera National Preserve (VCNP) at approximately 35·5 degrees north latitude in the Jemez Mountains of north–central New Mexico (Figure 1). This study focuses on an area of approximately 25 hectares on the eastern flank of Redondo Peak. The mountains within and around the preserve accumulate a continuous winter snowpack, which forms an important source of surface and groundwater for the surrounding semi-arid grasslands and deserts, as well as the upper Rio Grande which supplies the city of Albuquerque.

The VCNP as a whole is topographically complex, with a mean elevation of 2768 m (range 2167–3434 m) and mean slope of 12·8 degrees (maximum 75·4 degrees) (USGS, 2003). However, our research centres on an area with a range of canopy densities but relatively little variability in elevation and low slopes (Table I). Topography here is much more regular than in studies highlighting its importance in the distribution of snow in mountain catchments (Balk and Elder, 2000; Erxleben *et al*., 2002; Erickson *et al*., 2005; Geddes *et al*., 2005; Molotch *et al*., 2005). Geology of the VCNP is also complex, being primarily the result of a volcanic eruption and collapse around one million years ago which left Redondo Peak, a resurgent dome, and its surrounding crater covered with rhyolitic ash flow tuffs (Goff *et al*., 2006).

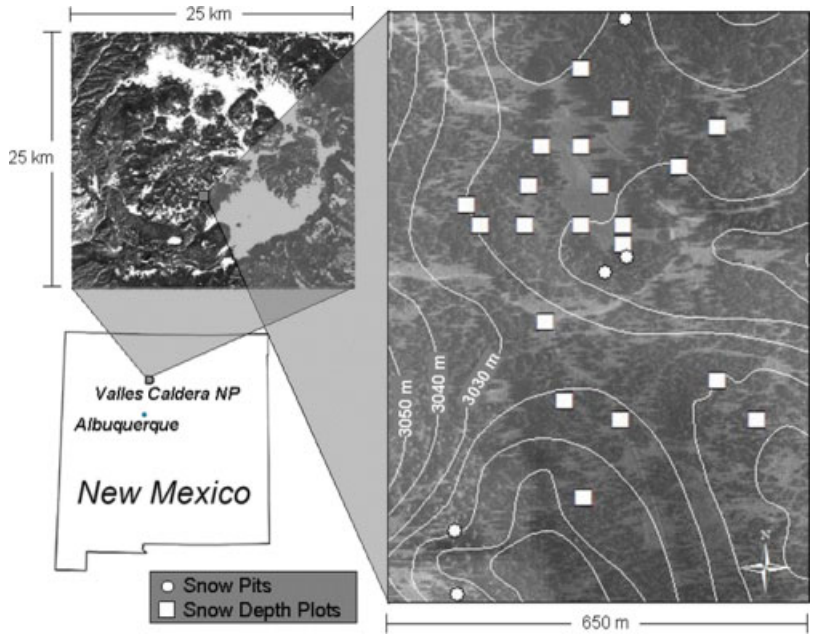

Figure 1. Location of research site within the Valles Caldera National Preserve (VCNP) of New Mexico. Squares represent 30 × 30 m intensive study plots and circles represent snow pit locations. The study area is characterized by variable forest density, low variability in elevation (~3015 m) and low slopes.

DOI: 10.1002/eco

Table I. Topographic characteristics of snow-depth measurement plots. Locations were chosen to maximize variability in forest properties while minimizing slope and elevation variability. Canopy density estimates are from the 2001 NLCD dataset (USGS, 2007); insolation was modelled in ArcGIS from a 10-m USGS DEM (USGS, 2003) and elevation and slope were extracted from the same DEM.

Forest class	(%) Canopy density	# Plots	# Datapoints	Elevation (m)	Slope (deg)	Solar (W/m^2)	Mean snow depth (cm)
Open	0	5	225	3014 ± 4	$3{\cdot}2 \pm 1{\cdot}5$	252 ± 3	$55{\cdot}4 \pm 9{\cdot}7$
Low	0–25	4	180	3018 ± 8	$4{\cdot}0 \pm 1{\cdot}4$	243 ± 7	$66{\cdot}0 \pm 3{\cdot}5$
Low–mid	25–50	4	180	3011 ± 7	$4{\cdot}0 \pm 3{\cdot}3$	252 ± 10	$60{\cdot}8 \pm 3{\cdot}1$
High–mid	50–75	4	180	3020 ± 12	$2{\cdot}9 \pm 1{\cdot}7$	240 ± 9	$42{\cdot}3 \pm 8{\cdot}9$
Dense	75–100	3	135	3018 ± 11	$4{\cdot}3 \pm 1{\cdot}3$	238 ± 15	$51{\cdot}0 \pm 12{\cdot}8$
Range	—	—	—	3004–3038	0·3–7·2	225–265	30·8–69·9

Wind data from a micrometeorological station, 1·8 km from the centre of this site, operating continuously since 2003, show a prevailing winter wind from the west–northwest (average direction for November through April of 287 degrees), with a mean winter wind speed of 2·0 m/s and a mean daily maximum wind speed of 7·2 m/s. These speeds are much lower than those found in studies showing wind to be an important factor in snow distribution (Hiemstra *et al*., 2002; Winstral *et al*., 2002). November through April precipitation at the same station averaged 40·9 cm between 2004 and 2007, while at the nearby Quemazon and Vacas Locas SNOTEL sites, November through April precipitation averaged 29·8 cm (1981–2006) and 32·34 cm (2002–2007), respectively. These precipitation values represent approximately 50% of the annual precipitation for the area, with the remainder falling as rain during the summer monsoon. Temperatures are warm for a mountain catchment; mean temperature from November through April for the years 1989–2006 was $-2{\cdot}3\,^{\circ}C$ at the aforementioned Quemazon SNOTEL site.

Vegetation type within the VCNP varies by elevation and soil type, with grassland in valley bottoms yielding to ponderosa pine at valley edges, which in turn gives way to a mixed conifer forest that covers all mountains in the preserve to their peaks. This study site is within and surrounded by a mixed conifer forest consisting mainly of blue spruce (*Picea pungens*), white pine (*Pinus strobiformis*), Douglas fir (*Pseudotsuga menziesii*) and white fir (*Abies concolor*) (Musselman *et al*., 2008). At an eddy covariance tower, 0·6 km from the centre of this study area, vegetation is dominated by Englemann spruce (*Picea engelmannii*) with mean height of 19·6 m, mean diameter at breast height (dbh) of 26·9 cm, mean leaf area index of 3·43 and mean stem density of 783 stems ha^{-1} (McDowell *et al*., 2008).

FIELD METHODS

We developed and used a sampling scheme to quantify the effects of forest canopy density on snow depth at the stand scale while minimizing the influence of other factors known to control SWE (i.e. topographic variability). We chose 20 plots, each 30-m square, to perform an extensive snow-depth survey, selecting several plots from each quartile of canopy density (i.e. 0–25%, 25–50%, etc.) along with several unforested plots to ensure that we would capture the site's variability in canopy density and forest edges. We sampled snow depth at 45 locations within each plot on March 11, 2007, for a total of 900 snow-depth measurements. To isolate the effects of vegetation, we chose plots with similar elevations and minimal slopes (Table I). As one objective of this study was to evaluate ways to make remotely sensed forest canopy information useful in water management, we positioned each 30-m plot to coincide with a Landsat pixel of known canopy cover as published in the national land cover database—forest canopy dataset (USGS, 2007) and used this dataset for canopy density estimates.

We adapted the sampling scheme within each 30-m plot from schemes used by Erxleben *et al*. (2002) and Cline *et al*. (2001) to produce a stratified random sample of snow-depth measurements, ensuring that samples would be roughly evenly dense across the sample space while minimizing bias (Figure 2). This scheme consisted of subdividing each plot into nine 10-m square sub-plots, with five depth measurements in each. In each sub-plot, we took one depth measurement at the centre and two each at 2 and 4 m from the centre, forming two orthogonal transects with 2-m spacing (Figure 2). We determined the orientation of these transects by random number generator. We navigated to each plot by map and compass, as well as Global Positioning Satellite receiver, carefully entering each sub-plot from a direction that would not intersect the depth measurement transects. At each sampling location, we measured snow depth to the nearest centimetre using a graduated aluminium hand probe inserted vertically into the snowpack to the ground surface.

To collect measurements of snow density we sampled six snow pits, located in a variety of forest canopy densities, on March 10, 2007 using the method described by Cline *et al*. (2001). Fewer snow density measurements were necessary than snow-depth measurements because variability in snow density is known to be conservative relative to depth (Elder *et al*., 1998). We excavated each pit to the ground surface, taking snow density, grain type and size, and temperature measurements at 10-cm vertical increments. We determined values of snow density by

DOI: 10.1002/eco

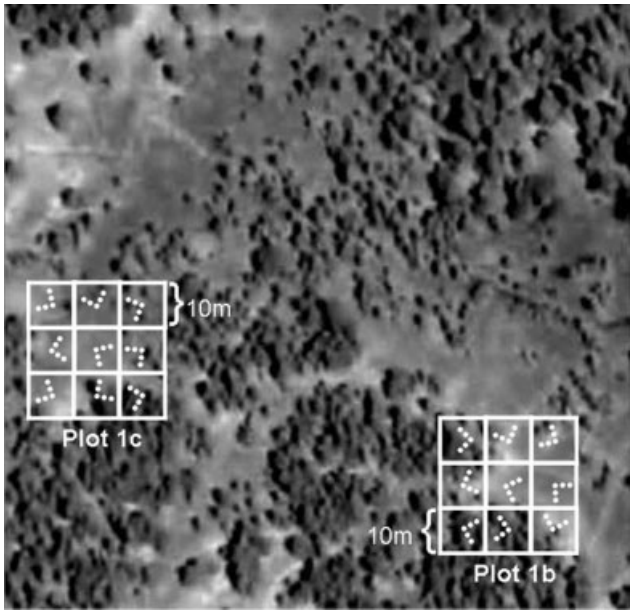

Figure 2. Example locations of depth measurements (white dots) within two of the twenty 30 × 30 m plots sampled for this work. Five depth measurements were obtained along orthogonal transects within each 10 × 10 m sub-plot.

extracting duplicate 1-L volumes of snow from each 10-cm interval with wedge-shaped stainless steel cutters and weighing them in the field, taking the average of the two masses to represent the snow density for that interval and taking the average of all intervals to represent the snow density for the pit. To avoid direct insolation of the sampling wall, we dug each pit so that the pit face was oriented away from the sun at the time of sampling.

MODELLING METHODS

Geographic information system (GIS)-based modelling of solar radiation

To investigate the effects of forest density on snowpack insolation and to generate values of below-canopy insolation for statistical modelling (described in the two sections below), we modelled solar radiation for various forest densities using synthetic random forests within a geographic information system (GIS). Several aspects of forest canopy structure, including density, patterns of gaps and tree species, interact to exert strong influence on solar radiation transmittance to the snowpack (Hardy *et al*., 2004); we sought to create as simple a representation as possible to assess the relationship between canopy density and snowpack solar loading. We approximated each tree as an opaque right cone with 15-m height and 3-m radius and placed them randomly within 30-m square domains, reproducing the forest densities of the 20 plots we measured in the field. We used a Monte Carlo method to calculate the area and thus the canopy density of each random forest: we placed 100 000 random points in each forest, with the percentage of these that intersect trees being equal to the canopy density. We then used these hypothetical forests to generate a digital elevation model with 10-cm cell size to reflect the conical trees where they exist and the mean elevation of the study site (3015 m) at all other points. Finally, we used the Solar Analyst tool (Fu and Rich, 2000) within the Spatial Analyst extension of ArcGIS 9·2 software to model the direct and diffuse insolation to each horizontal cell (i.e. ignoring insolation to the trees themselves) within the analysis extent (Figure 3 for an example).

In addition to modelling insolation for each of the canopy densities sampled in the field, we modelled forests of 90 and 95% density, to provide information about the likely effects of very dense forests that are not currently common at our site. We replicated each density five times in random orientations to avoid bias from anomalous forest orientations and normalized insolation values to a scale of zero-to-one by dividing each value by the value generated for a flat, treeless surface.

Binary regression trees

A binary regression tree is a non-linear, hierarchical statistical model in which a dataset of dependent variable values is recursively partitioned into increasingly homogeneous subsets (Breiman *et al*., 1984; Clark and Pregibon, 1992). We constructed binary regression trees to model snow depth as a function of topographic and vegetation variables to determine the relative importance of each variable on snow depth and to evaluate whether

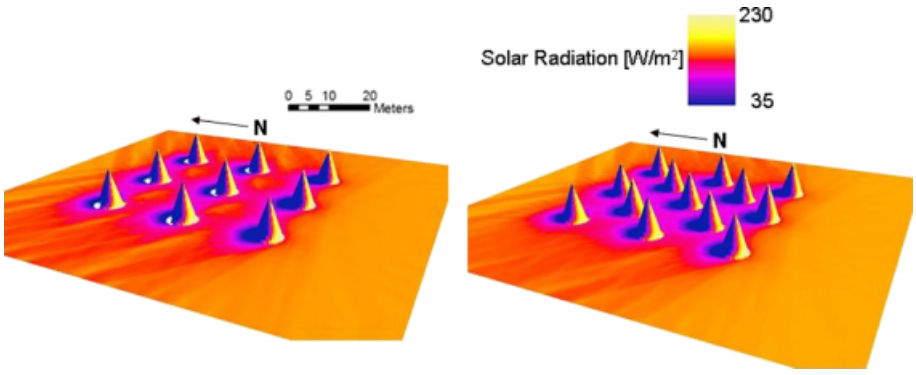

Figure 3. Two examples of modelled solar load based on forest densities. The forest patch on the right, with canopy density of 16%, shows more shaded area than the patch on the left, with 12% canopy density. Examples use non-random tree positioning for display purposes.

DOI: 10.1002/eco

the addition of vegetation information can improve estimates of snow distribution. Non-linear statistical techniques such as binary regression trees are preferable to linear regression when non-linear relationships exist between the dependent and independent variables, as is frequently the case with snow depth. Tree models are also more adept at capturing interactions between variables, do not require assumptions of the form of variable interaction and can be used to indicate which independent variables are most important, since these will be utilized earlier in the recursive partitioning and thus will appear higher in the tree, closer to the root node. The use and effectiveness of binary regression trees in predicting spatial patterns of snow depth is well documented (Elder *et al*., 1998; Balk and Elder, 2000; Erxleben *et al*., 2002; Winstral *et al*., 2002; Molotch *et al*., 2005; Musselman *et al*., 2008). In this study, we intentionally created models to over-fit the data and then pruned them to optimal size as described in Clark and Pregibon (1992), choosing as optimal the model with the lowest overall mean deviance based on 100 iterations of ten-fold random cross-validation (see Molotch *et al*., 2005 for details of this procedure). Detailed descriptions of binary regression tree growing and fitting procedures may be found in Breiman *et al*. (1984) and Clark and Pregibon (1992).

Our tree models employ eight variables: elevation, slope, aspect, northness (the product of the cosine of aspect and sine of slope, see Molotch *et al*. (2005) for a detailed description and application), above-canopy solar radiation (modelled in ArcGIS 9·2 using the same Digital Elevation Model (DEM) (USGS, 2003) used to extract elevation, slope, and aspect), below-canopy solar radiation (the product of above-canopy solar radiation and normalized modelled shading as described in the previous section), forest canopy density from the 2001 national land cover database (NLCD) (USGS, 2007) and forest edgeness, which is the northness metric applied to the canopy density field instead of an elevation field and is intended to capture forest edge effects. Edgeness, in other words, is the product of the cosine of the direction (from north) of negative forest canopy gradient and the sine of the gradient {i.e. $\cos[\text{aspect}(-\nabla C)]\sin(\nabla C)$, where C is the forest canopy density field}. We borrow the term edgeness (edge strength) from the pattern recognition literature (e.g. Tolt, 2003), using it in a related though not strictly equivalent context.

Independent evaluation of combining remotely sensed data with regression tree modelling

In addition to constructing binary regression tree models of snow distribution at our site, we used an independent dataset to investigate the utility of adding remotely sensed forest canopy data to non-linear statistical models of snow distribution. This was necessitated by the low topographic complexity at our site, which may limit the applicability of models developed with our field data but does not necessarily affect the value of our techniques. For our independent data, we chose the intensive study area (ISA) snow depth transects dataset collected during the NASA cold land processes experiment (CLPX). The CLPX was a multi-scale, multi-sensor experiment designed to extend local-scale understanding of snow and ice related processes to regional and global scales. The ISA portion of the experiment, in which over 8000 snow-depth measurements were taken during the spring of 2002 and over 11 000 depth measurements were taken in the spring of 2003, was designed to investigate variability in snow distribution at remote sensing scales (Cline *et al*., 2002, updated 2003). These depth measurements were taken in nine-square ISAs in north–central Colorado, each 1 km^2, ranging in elevation from 2460 to 3670 m and extending over 95 km from their southernmost to northernmost point. Topography for the ISAs ranges from low-to-moderate, with a wide range of vegetation types including treeless dry grasslands, riparian areas, low-to-high density coniferous and deciduous forests, sub-alpine coniferous forest and alpine tundra (Cline *et al*., 2001). As in the current study, we focused on processes from the maximum accumulation season, in this case corresponding to data collected during the second campaign of each season, between March 25 and 29 of both years. In addition to using regression trees to model the entire dataset for these time periods, we also modelled four specific ISAs due to their high variability in topographic and forest canopy variables, namely, the Fraser Alpine (FA), Rabbit Ears—Spring Creek (RS), Rabbit Ears—Walton Creek (RW) and Rabbit Ears—Buffalo Pass (RB) transects. Average elevations for areas FA, RS, RW and RB are 3567, 2788, 2950 and 3161 m, respectively, and dominant vegetation types consist of alpine tundra with some coniferous forest, moderate density deciduous forest, meadow with small stands of coniferous forest and dense forest interspersed with meadows, respectively. More detailed description of the experiment sites and methods are available in Cline *et al*. (2001). For each of these snow-depth datasets, we constructed binary regression tree models using the same methods and variables as described in the previous section, extracting canopy density data from the NLCD 2001 dataset (USGS, 2007), topographic data from the National Elevation Database (USGS, 2008) and snow depths from the Digital Atlas of Cline *et al*. (2001). Following Winstral *et al*. (2002), we modelled snow depth rather than SWE for this dataset, assuming that SWE would follow roughly the same patterns as depth due to the substantially smaller variability in snow density than in depth.

As described in the Section on Methods for binary regression trees, we employed eight variables in statistical modelling of this dataset: elevation, slope, aspect, northness, above-canopy and below-canopy solar radiation, forest canopy density and forest edgeness (the cosine of the aspect of negative forest gradient times the sine of the gradient). As with the binary regression tree models described in the previous section, we derived the first four of these parameters from a 10-m USGS DEM (USGS, 2008), while we derived the last four from the forest canopy density data in the 2001 NLCD (USGS,

DOI: 10.1002/eco

2007). With the exception of edgeness, each of these independent variables has been used in prior modelling of spatial patterns of snow distribution (Wigmosta *et al*., 1994; Balk and Elder, 2000; Erxleben *et al*., 2002; Winstral *et al*., 2002; Geddes *et al*., 2005; Molotch *et al*., 2005; Musselman *et al*., 2008).

Energy and throughfall-based modelling of net snow accumulation in forests

On the basis of our findings showing the significant effects of forest density and edges on snow depth (presented in the Section on Results), we hypothesized that forests with moderate canopy densities hold the greatest snow depths due to the large amounts of shaded open area, but relatively little canopy interception associated with these densities. To test the plausibility of this mechanism, we created a simple model based on the four distinct energy/throughfall regimes shown in Figure 5b: under canopy, corresponding to high interception and low energy; open, corresponding to little interception and high energy; shaded open, corresponding to low interception and low energy; and south forest edge, corresponding to a regime with interception, high energy, and possibly high longwave re-radiation. As in the Section on GIS-based Solar Radiation Modelling, we assumed randomly oriented 15-m high trees at a latitude of 35·5 degrees and used a Monte Carlo approach to determine the relative contributions of each regime type to the total area of a 30-m square plot as a function of forest canopy density. Determining the geometric boundaries of each regime is necessarily subjective—we chose to define under canopy as strictly equal to canopy density, shaded open as the shadow cast by a tree at one instant in time (specifically solar noon on Julian day 39, midway between the winter solstice and our sampling date), south forest edge as a region extending from the southern quarter of each tree canopy edge to 1 m from the edge and open as the remaining area. Though the south forest edge regime is intended to include both interception and insolation and therefore might be constrained only to southerly, unshaded, under canopy areas, we extended it 1 m beyond the canopy as a conservative measure to account for the possibility of increased longwave radiation reducing snow depth in that region as shown by Musselman *et al*. (2008). We then applied the observed snow depths shown in Figure 5b and appropriate estimates of snow density (an average of mean snow densities from the two forested snow pits for the 'under canopy' classification, an average of mean snow density from the four unforested snow pits for all other classifications) to each of the four regimes and defined an area-weighted average of these as modelled SWE for that 30-m square plot, yielding an estimate of average water equivalent as a function of canopy density.

RESULTS

Meteorological observations

During the 2006–2007 water year under study, snowpack accumulation began on October 23, 2006. As much as 25·5 cm of precipitation was recorded between this date and the snow-depth survey date of March 10. Adjusting this value for wind-induced undercatch using the method of Goodison (1998) yielded a total of 28·8 cm of precipitation (Table II), representing approximately 32% of the total precipitation that water year. Maximum SWE was 107 and 115% of the long-term averages at the nearby Quemazon (1981–2007) and Vacas Locas (2002–2007) SNOTEL sites, respectively, while average temperature from November to April was −0·17 and −0·42 °C at the same two sites. Mean winter wind direction for the season studied here was 290 degrees, with wind originating between 270 and 345 degrees 66·4% of the time. Mean wind direction during hours with recorded precipitation between October 23 and March 10 was 295 degrees, while mean wind direction during hours of relative humidity greater than 75% (possible precipitation and/or blowing snow events) was 297 degrees. Mean wind speed for this season was 1·9 m/s, with mean hourly maximum wind speed of 4·4 m/s and overall maximum wind speed (3 s) of 14·4 m/s. Mean wind speed during hours of recorded precipitation and during hours of high relative humidity were 2·0 and 1·9 m/s, respectively.

Stand-scale snow-depth surveys

Snow-depth data collected in 20 plots of various forest densities during maximum accumulation season shows

Table II. Meteorological data for the winter under study (water year 2007) and longer-term datasets. The winter under study was warmer than the long-term average but precipitation, wind, and snow accumulation were similar. Winter season is defined as October 28 (day of first snow accumulation in water year 2007) through date of maximum SWE accumulation. Values listed for multiple years are means of those years.

Winter season	Quemazon SNOTEL			Vacas Locas SNOTEL			VCNP local micro-met station and snow-depth sensors			
	Max SWE (cm)	Mean temp (°C)	Mean date peak SWE	Max SWE (cm)	Mean temp (°C)	Mean date peak SWE	Winter precipitation (cm)	Max depth (cm)	Mean wind speed (m/s)	Vector mean wind direction (deg)
1981–2006	25·7	−2·2	March 21	—	—	—	—	—	—	—
2003–2006	18·5	−2·1	March 16	23·9	−2·3	March 18	—	—	—	—
2005–2006	20·9	−2·0	March 16	25·1	−1·8	March 11	24·6	64	1·9	279
2007	27·4	−0·2	March 7	28·4	−0·4	March 6	28·8	72	1·9	290

DOI: 10.1002/eco

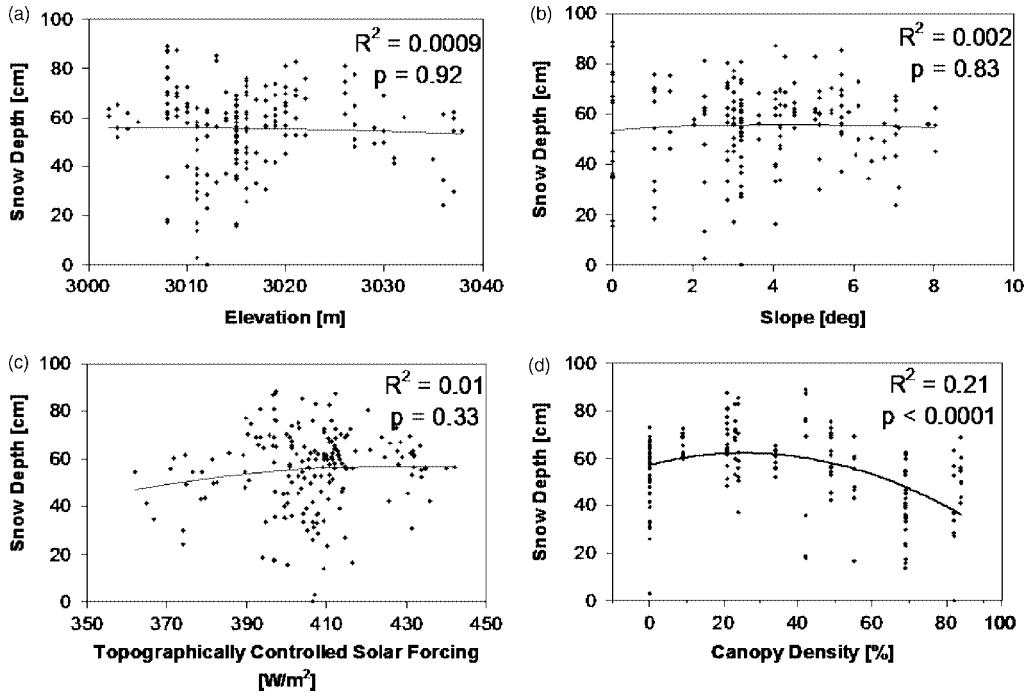

Figure 4. Mean snow depths in each 10 × 10 m sub-plot at maximum accumulation as a function of elevation (a), slope (b), topographically controlled (i.e. above-canopy) solar forcing (c) and NLCD forest density (d). Moderate forest density, with canopy coverage between 20and 40%, is associated with greater snow depths than either open areas or dense forest.

that deeper snow accumulated in forests of moderate canopy density than in either open areas or in dense forests (Figure 4d). Snow in these forests was about 8% deeper than in open areas. In contrast to the correlation between forest density and snow depth, no strong influence on snow depth was evident for elevation, slope or solar index (Figure 4a–c).

Analysis of snow depths at forest edges showed that southern edges of forests accumulated an average of 46% less snow than forested areas without southern edges (30·7 and 57·0 cm, respectively), while open areas immediately to the north of forests accumulated 26% more snow than open areas without such an edge (74·1 and 58·9 cm, respectively, Figure 5b). Western edges of forests and open areas, oriented perpendicular to the predominant westerly wind direction, did not contain significantly different snow depths than forests or open areas without western edges (Figure 5a).

Snowpack characteristics

The six snow pits ranged in mean density from 288·2 to 363·9 kg/m^3, with a mean of 324·3 kg/m^3. Densities were generally consistent within each pit; standard deviations of density among layers of the same pit ranged from 17·8 to 27·4 kg/m^3. Snow temperatures for each snow pit layer ranged from −2·5 to −0·5 °C, with means and standard deviations of temperatures within pits ranging from −2·8 to −1·3 °C and from 0·2 to 1 °C, respectively (Table III). All snow pit layers had temperatures below 0 °C. In each pit, between two and five distinct sun crusts were clearly visible, with rounded crystals and decomposing dendrites between them at various depths and between 4 and 13 cm of depth hoar at the base. Because solutes near the top of a melting snowpack are known to elute before those in other layers (Bales *et al.*, 1989), a roughly consistent distribution of solutes throughout a pack may be taken as evidence that melt has not yet begun. Continuity in snow crystal stratigraphy and chemical concentrations between and within pits indicated that no melt had occurred at the pit sites before our sampling date (Table III; please see Gustafson *et al.* (in preparation) for a detailed description of solute concentrations in these snowpits).

In light of the significant differences in snow depth we found associated with forest edges as described above and shown in Figure 5b, we used snow density values associated with the four energy and deposition regimes identified in the snow-depth survey to distribute estimates of snow density and convert snow depths to water equivalent. For each depth measurement location, we calculated SWE using a weighted average snow density:

$$\mathrm{SWE} = d(C\rho_c + C_S\rho_S + O\rho_o + O_N\rho_N) \qquad (1)$$

given

$$C + C_S + O + O_N = 1 \qquad (2)$$

where C, C_S, O and O_N are the fractional areas covered by canopy, south edge of canopy, open and open just north of canopy, respectively, and ρ_c, ρ_S, ρ_o and ρ_N are snow densities for the same four classifications. The relative contribution of each category to a total area depends on solar angle and canopy structure; we defined each fraction as a function of canopy density as described above in the context of energy and depositional regime modelling. Using this formulation with the best available representative snow densities for each classification (the mean snow density of the unforested pit with the greatest

DOI: 10.1002/eco

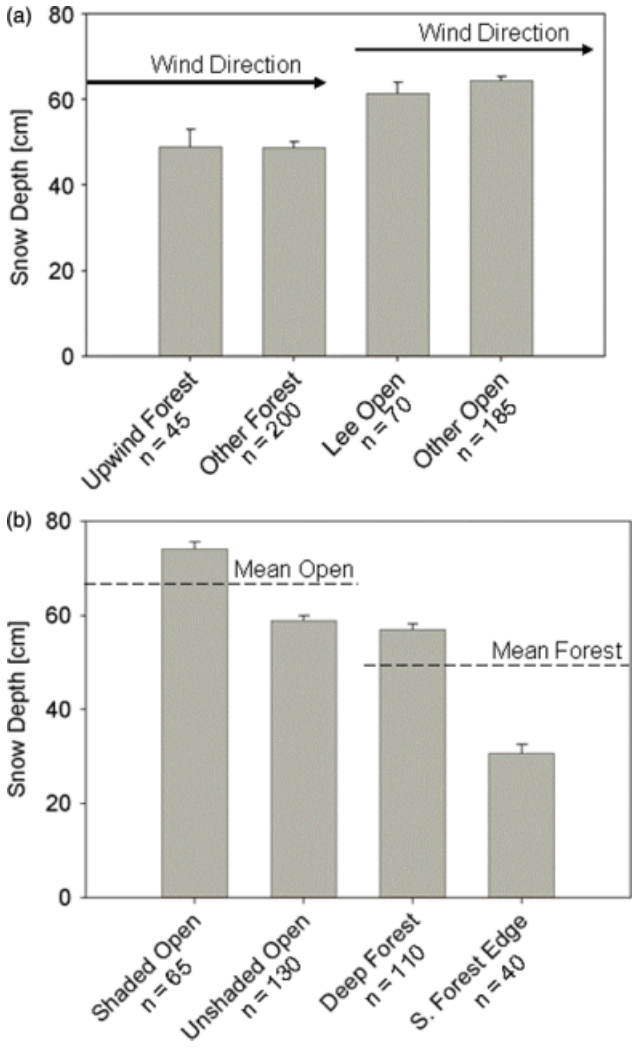

Figure 5. Maximum individual snow depths as function of forest edge orientation. East–west edges (a) suggest wind redistribution has little effect on depth at our site; north–south edges (b) in contrast, exhibit a pronounced gradient with greatest snow depth in shaded, open areas on the north side of forest patches, similar snow depths in unshaded open and contiguous forests, and shallowest snow depths on the immediate southern edges of forest patches.

degree of solar radiation shading for ρ_N, the average snow density of the two snow pits in forested areas for ρ_c and ρ_S and the average snow density of the four pits in clearings for ρ_o), resulted in a similar pattern for SWE as a function of canopy density as shown for depth in Figure 4: maximum accumulation was associated with canopy density between 20 and 40%, with peak accumulation approximately 7% greater than in open areas.

Stand-scale GIS modelling of solar radiation in forests

Modelled solar radiation shows a strong correlation with forest canopy density ($R^2 = 0{\cdot}94$, Figure 6). Insolation to the horizontal plane (hypothetical snow surface) decreases with canopy density, generally following an exponential decay pattern. At approximately 45% canopy density, diffuse (atmospherically scattered) radiation overtakes direct radiation as the major form of insolation, under the assumption of generally clear-sky conditions. Comparison of total modelled insolation using this GIS-based approach to the common practice of using Beer's Law to estimate shortwave transmittance through forest canopies (Wigmosta *et al.*, 1994; Berbigier and Bonnefond, 1995; Wang, 2003), following Pierce and Running (1988) in using 0·52 as an average light extinction coefficient for conifers, resulted in a high degree of correlation ($R^2 = 0{\cdot}95$) between the two methods.

Binary regression trees

Application of the binary regression tree technique to our dataset resulted in minimum model deviance for a tree

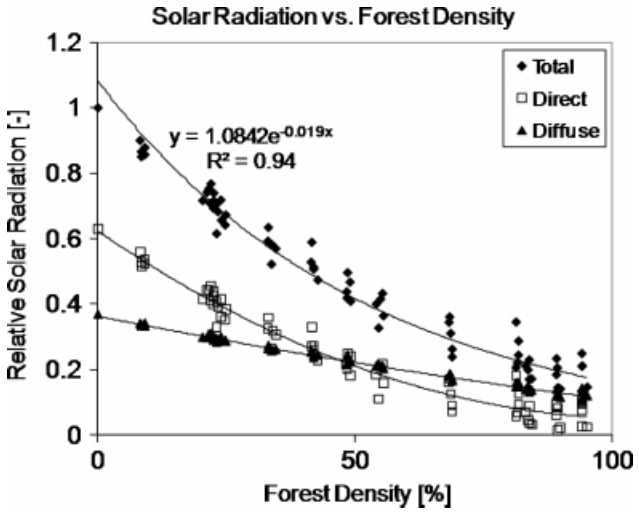

Figure 6. Normalized solar index as a function of forest density. Solar radiation decreases exponentially with increasing canopy density, with diffuse radiation becoming the dominant component at approximately 45% canopy density.

Table III. Basic characteristics of the six snowpits sampled for this study. VWM refers to volume weighted means. Please see Gustafson *et al.* (in preparation) for a more thorough investigation of spatial patterns of snow chemistry and isotopes at this site.

Snowpit	Forest cover	Temp. (°C)		Snow density (kg/m^3)		Cl^- (μeq/L)		SO_4^{2-} (μeq/L)	
		Mean	σ	VWM	σ	VWM	σ	VWM	σ
NL	Open	−1·3	0·3	315·9	25·3	17·4	10·0	10·6	8·3
SL	Open	−1·6	0·7	363·9	24·9	19·2	5·6	12·5	6·2
T	Open	−1·9	0·2	335·9	20·8	19·0	3·8	13·1	8·7
LR	Open, shaded	−2·3	1·0	313·3	25·5	19·7	7·1	11·6	5·3
SC	Forest	−2·8	0·2	328·7	17·8	17·8	9·0	9·7	5·6
DV	Forest	n/a	n/a	288·2	27·4	26·9	17·7	13·5	2·2

DOI: 10.1002/eco

with 12 terminal nodes (Figure 7), yielding an R^2 of 0·51. Adding the forest density and forest edgeness variables lowered mean model deviance from 40587 to 39542, slightly increased R^2 from 0·48 to 0·51 and increased optimal tree size from 10 terminal nodes to 12, relative to using topographic variables alone. Examination of the optimally pruned model shown in Figure 7 shows that shallower snow depths are associated with western aspects, a finding that is consistent with predictions by Rinehart *et al*. (2008), who showed that areas with high land-view factors can receive significantly increased energy in the form of reflected shortwave radiation when the land surface is snow-covered. At this site, on the eastern flank of Redondo Peak, western aspects have significantly greater land-view factors than eastern aspects. After aspect, the next most important factors in this model are above-canopy insolation and forest edges, with greater snow depths associated with less insolation and high edgeness (i.e. northern edges of forests), highlighting the importance of solar radiation on snow depth at this site and of forest edges on patterns of snow accumulation.

Applying the same technique to the CLPX dataset was also successful: in nine of ten cases, the addition of remotely sensed vegetation information improved model performance over the use of remotely sensed topographic information alone (Table IV). The edgeness, canopy density and below-canopy insolation metrics were each employed by at least four models, with all three metrics employed by three of the ten models. In most cases, improvement in model R^2 with the addition of forest canopy metrics derived from remote sensing was comparable to the effect of utilizing a field-gathered categorical canopy variable ('Cnpy'). Because field-gathered variables cannot be used to distribute estimates of snow depth at the catchment scale, this is a significant finding for improving estimates of snow distribution at watershed scales.

Energy and throughfall-based modelling of net snow accumulation in forests

Modelling the average SWE in a forest plot as a function of the relative areas contributed by the four energy and throughfall regimes identified in the snow-depth survey indicated peak SWE would be expected at a canopy density of 34%, with about 6% more SWE at this density than in an unforested area (Figure 8). As the proportion of the plot covered by forest canopy increases, unshaded intercanopy area decreases roughly exponentially, while shaded open and south forest edge areas follow a concave-down pattern, peaking at canopy densities of 47 and 44%, respectively.

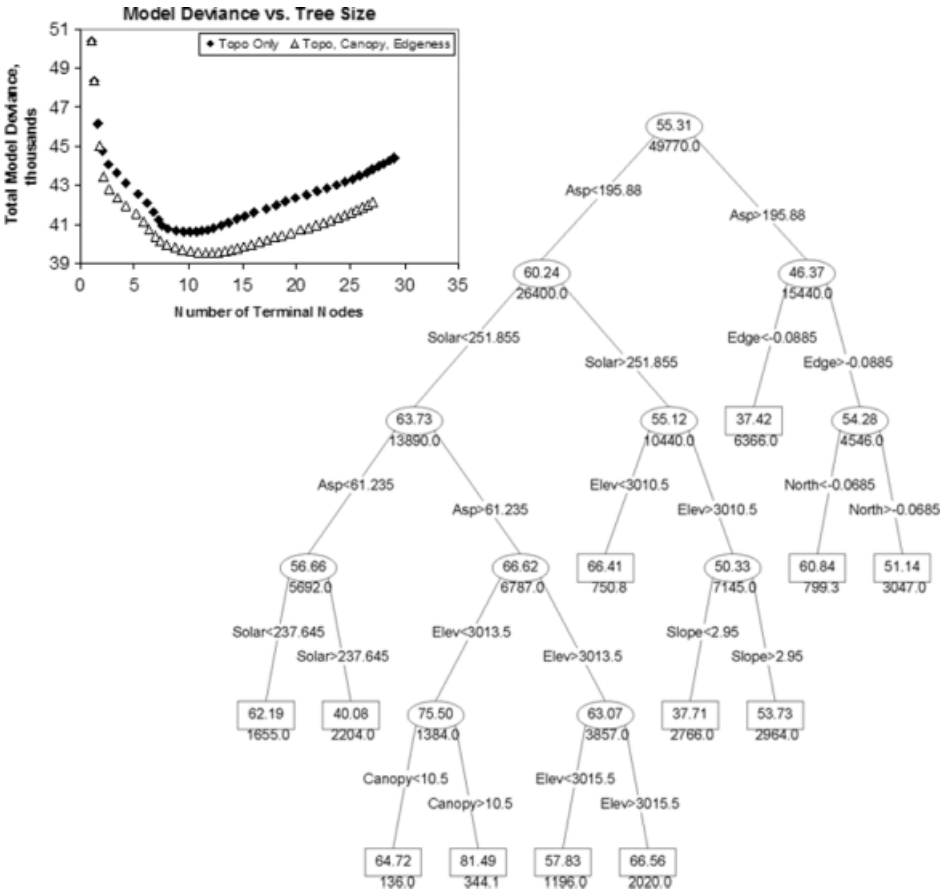

Figure 7. Optimized binary regression tree model of snow depth as function of forest density, forest edgeness, elevation, slope, aspect, northness and solar index. Upper left graph shows how model deviance varies with size, optimizing at 12 terminal nodes. Model performance improved with the addition of forest canopy variables (forest density and edgeness) over the model with only topographic variables (elevation, slope, aspect, northness and above-canopy solar radiation).

DOI: 10.1002/eco

Table IV. Effects of adding remotely sensed forest canopy information to binary regression tree models of snow depth from the March 2002 and 2003 CLPX datasets. In all but one case, adding forest canopy information improved model performance, generally to a similar degree as adding 'Cnpy,' a field-gathered vegetation variable. 'Best model' refers to the cross-validated regression tree that minimizes model deviance for each dataset, using remotely sensed topographic and forest canopy information.

CLPX dataset	Topo only R^2	Best model R^2	Best model parameters	Topo + Cnpy R^2
All 3/2002	0·860	0·877	Topo + Canopy	0·876
All 3/2003	0·900	0·907	Topo + Canopy	0·900
3/2002 FA	0·648	0·673	Topo + Canopy	0·683
3/2002 RW	0·198	0·247	Topo + TotalSol	0·281
3/2002 RS	0·361	0·418	Topo + Canopy, Edgeness, TotalSol	0·476
3/2002 RB	0·176	0·146	Topo + Canopy	0·264
3/2003 FA	0·661	0·689	Topo + Canopy, Edgeness, TotalSol	0·701
3/2003 RW	0·307	0·352	Topo + Edgeness	0·339
3/2003 RS	0·402	0·474	Topo + Edgeness	0·554
3/2003 RB	0·341	0·367	Topo + Canopy, Edgeness, TotalSol	0·360

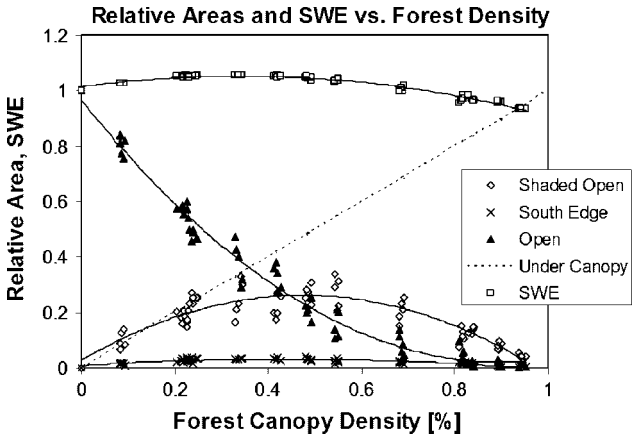

Figure 8. A simple energy-interception model of SWE (□) calculated using observed snow depths and densities multiplied by the fractional area of shaded open (◊), unshaded open (▲), deep forest (- - - -) and south forest edges (×).

DISCUSSION

Data from a stand-scale snow-depth survey and a statistical model show that in a high solar load environment typical of water source areas in the southwest, forest density and geometry significantly influence patterns of net snow accumulation. Forest edges, in particular, exert strong control over snow depth, with unforested areas shaded by vegetation to their immediate south holding much deeper snow than either deep forest or large clearing areas, and forested areas exposed to solar radiation through open areas to their immediate south holding much less snow. These findings agree with those of Kuz'min (1960, cited in Gelfan *et al.* (2004)) and Golding and Swanson (1978, 1986), who documented that the distinct energy and throughfall regimes created in forest openings and edges result in snow depths that differ predictably from either large open areas or areas of dense canopy. Golding and Swanson (1986), for example, found that northern edges of clearings at Marmot Creek, Alberta, receiving more direct solar radiation than southern edges, held up to 52% less snow than southern edges, a discovery consistent with our findings shown in Figure 4.

These findings also indicate that forests with moderate canopy densities, through significant shading of the snowpack but only marginal interception of snowfall, create a large number of small shaded openings that result in more snow on average than in either open areas or denser forests. We tested the plausibility of this mechanism in a model of energy and throughfall regimes as a function of forest canopy density and found good agreement with field data. As forest canopy increases, under-canopy areas slowly come to dominate the overall area, tending to replace open areas first, then shaded open areas as these become more common. As a result, modelled SWE follows a concave-down parabolic trajectory, peaking in forest with approximately 34% canopy density. Modelled SWE does not exactly match the pattern observed in field data, which peaks at approximately 25% forest density, but the shape is the same and the effect magnitude similar, with maximum modelled SWE about 6% more than in open areas while maximum observed SWE is about 7% more than in open areas.

Spatial patterns of SWE are important for hydrological and ecological studies because they are proxies for patterns of spring meltwater input to the catchment, provided that they are not the result of melt themselves. Data from six snow pits at our site show that melt had not yet begun when we conducted our snow-depth survey. The existence of multiple distinct sun crusts in each pit, separating layers of round and dendrite crystals in various stages of decomposition, along with snow temperatures below 0 °C for every sampled layer, are strong indicators that melt had not begun. Furthermore, no physical melt indicators in the form of liquid water, flowpaths or 'fingers' of ice were found at any of the six pits. Solute concentrations within each snow layer also suggest a snowpack that had not yet experienced melt. Bales *et al.* (1989) showed that if snowmelt progresses to the point that water leaves the bottom of the pack, solutes are flushed out with the water and their concentrations within the pack decrease rapidly, while if melt begins and ends sporadically, without resulting in water leaving the pack, solutes are moved within the pack and their concentrations vary dramatically between snow layers.

DOI: 10.1002/eco

Our six pits show low variability in solute concentration between sites and between layers, indicating that no meltwater had left the pack or moved within it (Table III; please see Gustafson *et al*. (in preparation) for a complete description of snow isotopes and chemistry from these pits). We can therefore be confident that lower snow depths associated with higher energy regimes are due to sublimation and thus do represent patterns of spring meltwater input to the catchment.

Examination of the binary regression tree model shown in Figure 7 highlights the processes controlling snow depth at our site. The first split in the tree divides the dataset into east and west aspects, with western aspects holding shallower snowpacks. Lesser snow depths on western aspects have been reported in other studies (Erxleben *et al*., 2002; Geddes *et al*., 2005), suggesting that this may be a widespread property of snow distribution patterns, potentially related, for example, to warmer air temperatures during afternoons while western aspects receive direct insolation. This finding also agrees with Rinehart *et al*. (2008), who showed that reflected shortwave radiation from snow-covered hillslopes and vegetation can result in significant redistribution of energy to facing slopes with high land-view factors, which is the case for western aspects at this site, being on the eastern flank of Redondo Peak. A detailed study would be needed to test these possibilities at our site, but if evidence for either or both could be found it would again highlight the importance of solar radiation on patterns of snow depth. An alternative explanation involves wind redistribution: winds at this site are consistently from the west, meaning western aspects are more exposed to wind scour (Winstral *et al*., 2002). However, wind speeds at this site are low, typically not reaching the 5–10 m/s needed to induce saltation of snow (McClung and Schaerer, 2000). Furthermore, the relatively warm temperatures and high solar loads found at this site lead to snow surface hardening, requiring even greater wind speeds to induce redistribution, and the frequent stands of vegetation make the long fetches needed for equilibrium drifting scarce.

After aspect, the next decisions in the tree model are related to (above-canopy) solar radiation and forest edges. The prominence of solar radiation again emphasizes the importance of that variable for snow depth, while the edgeness metric clearly shows the effect of forest edges. Like northness, edgeness (the product of the cosine of the direction of negative forest canopy gradient and the sine of the gradient) ranges from −1 to 1, with high values indicating areas where forest canopy is losing density rapidly in the northward direction, highly negative values indicating rapid loss of canopy density in the southward direction and values near zero indicating little variation in density and/or east–west gradient. Greater snow depths in this model are clearly associated with northern forest edges (high edgeness), confirming the findings of Figure 4.

As shown in Figure 7 and Table IV, the addition of remotely sensed forest canopy information improved regression tree model performance for both this study and for the 2002–2003 CLPX study. In the case of the CLPX dataset, the addition of remotely sensed canopy information improved model performance for nine of ten datasets and generally increased model R^2 by a comparable amount to the addition of Cnpy,' a categorical vegetation cover variable gathered in the field. This is significant because field-gathered variables are not available for distributing estimates of snow depth and water equivalent throughout a basin, and because the 'Cnpy' variable includes two categories corresponding to tree canopies containing intercepted snow, an additional degree of information unavailable to the remotely sensed forest canopy dataset. Furthermore, model improvement with the addition of below-canopy radiation, forest canopy density, and edgeness (all derived from 2001 NLCD data) shows that these also exert influence on patterns of snow distribution in the CLPX dataset, broadening the applicability of our depth survey findings beyond the boundaries of our field research site. Though initial improvements in model R^2 may appear modest, a complete evaluation of this modelling method will require further model development beyond the scope of this paper, including techniques such as spatial distribution of model residuals (Balk and Elder, 2000; Molotch *et al*., 2005). As a proof of concept requiring further technique refinement, these findings are highly encouraging for using remotely sensed vegetation data to improve models of spatial distribution of snow, particularly given that new capabilities for remote detection of vegetation cover are under development (National Research Council, 2007).

Because the binary tree growing algorithm recursively splits a dataset using the best available variable information, it would seem that providing additional information would always improve model performance. As shown in Table IV and demonstrated by Molotch *et al*. (2005), however, this is not the case. Seven of the ten CLPX datasets were modelled more effectively without access to all variables; in one of these, the optimal model used topographic information only. When an additional variable allows the regression tree model to split the dataset such that model deviance is minimized more quickly, it will do so, regardless of whether this addition eventually reduces model deviance overall. Molotch *et al*. (2005) addressed this by manually rebuilding and comparing regression tree models created using every combination of independent variables. As the size and dimensionality of datasets becomes larger with increasing information availability, this approach becomes less tractable, so we recommend that an investigation be made into methods of determining the optimal amount of information to provide to statistical models of snow distribution.

Modelling snowpack insolation within a GIS environment showed similar results for total insolation to the Beer's Law methodology used in previous studies (Wigmosta *et al*., 1994; Berbigier and Bonnefond, 1995; Wang, 2003), demonstrating that this procedure is effective even as it is much simpler than optics-based methods such as GORT (Li *et al*., 1995) which require specific

DOI: 10.1002/eco

canopy structure parameters. In contrast to Beer's Law-based estimates, however, the GIS-based method used here allows adjustment of parameters such as tree height, latitude, canopy geometry and seasonality with corresponding impacts on snowpack shading. This method also reveals greater data dispersion at higher canopy densities, illustrating the relatively greater impacts of edge effects and canopy geometry in dense forests and differentiates between direct and diffuse radiation components [direct and diffuse radiation transmission can also be found using Beer's Law, but only if light extinction coefficients are known for both (Wang, 2003)]. Though there are many simplifying assumptions implicit in the GIS-based method, it provides a starting point for future work investigating the impacts of forest patch orientation, banding and probabilistic distributions of canopy parameters.

Vegetation and topography combine in complex, interacting processes to determine spatial patterns of snow depth in mountain catchments (e.g. McKay and Gray, 1981; Hiemstra *et al*., 2002; Geddes *et al*., 2005; Liston and Elder, 2006). Careful examination of snow survey data and non-linear statistical models and investigation of alternative explanations for the observed pattern of snow accumulation lead to the conclusion that the combination of throughfall and solar radiation is the simplest and most likely explanation for finding maximal snow accumulation associated with moderate density forest canopy. Figure 9 shows interception, derived from Equations (10) and (13) from Pomeroy *et al.* (2002) and below-canopy insolation, from Figure 6, alongside measured and modelled values of SWE for this study site. The concave-down pattern of snow accumulation as a function of forest canopy density is consistent with a linear combination of interception (linearly increasing) and snowpack insolation (exponentially decreasing) subtracted from a constant precipitation value.

Future work in this area should include scenario analyses involving large-scale loss of forest cover due to insect infestation and/or fire, as these events have become increasingly common in recent years (Breshears *et al*., 2005; Westerling *et al*., 2006). Optimizing forest densities and configurations to control water input to the catchment should also be investigated further; in contrast to the well-studied impacts of timber harvesting on streamflow (Bosch and Hewlett, 1982; Ffolliott *et al*., 1989; Hornbeck *et al*., 1997), much remains to be learned in this area. The transferability of the findings of this study to other sites is unknown due to the specific topographic characteristics and the relatively little variability in tree species at this site; future study design should investigate these controls and test these proposed frameworks in a broader context, as well as investigate using these findings to distribute estimates of snow depth and water equivalent at the basin scale. Finally, the impacts of forest density and geometry on snowmelt timing must be explored, as the mountain snowpack represents a significant storehouse of water resources that may behave differently with changes in climate and vegetation. Coupled hydrologic and econometric models may be needed to help determine the overall change in value when both snowmelt quantity and timing are altered by vegetation change.

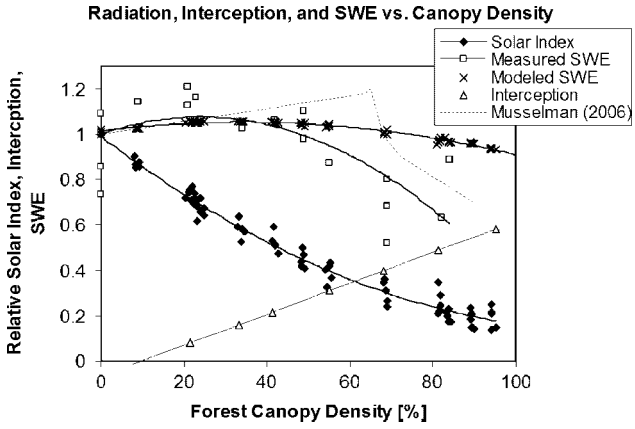

Figure 9. Comparison of the effects of forest density on measured SWE from this study (□) with predictions from the energy-interception model presented in Figure 8 (×) and Mussleman *et al*.'s model (2006) (- - - -). Solar forcing (♦) and interception (△) are presented for reference.

CONCLUSIONS

A detailed snow depth and density survey showed that forest canopy density significantly affects maximum snow accumulation at the stand scale. Snow depth and water equivalent were greatest in a forest with canopy density between 25 and 40%, having approximately 8 and 7% more snow than open areas, respectively. Forest edges also had significant influences on snow accumulation, with open areas immediately to the north of forest patches holding 26% more snow than either large open areas or dense forest areas and 140% more snow than southern forest edges. Investigation of alternative potential controls suggested that the combination of canopy interception and shading of the snowpack from direct solar radiation was the most likely cause of this result. Modelling of forest patches as collections of opaque right cones showed that insolation to the snowpack decreases exponentially with forest density; the combination of this response curve with the linearly increasing trend of snowfall interception is concave-down (Figure 9). Statistical models of the spatial distribution of snow depth improved with the addition of remotely sensed forest canopy information from the NLCD forest canopy dataset, (USGS, 2007), both in this study and in the independent CLPX dataset. The widespread availability of NLCD data makes these findings broadly applicable and testable throughout the conterminous United States.

ACKNOWLEDGEMENTS

This research was supported by SAHRA (sustainability of semi-Arid hydrology and riparian areas) under the STC Program of the National Science Foundation, agreements EAR-9876800 and EAR-0714054. We thank the students

DOI: 10.1002/eco

of the University of Arizona Spring 2007 HWR 696F Snow Hydrology Class and Dr Steven Fassnacht and his students from Colorado State University for their help with field data collection. We thank Scott Gilmore of SAHRA and the VCNP for field work and for a mathematical approximation of the overlapping areas of multiple shapes.

REFERENCES

Bales RC, Davis RE, Stanley DA. 1989. Ion elution through shallow homogeneous snow. *Water Resources Research* **25**(8): 1869–1877.

Balk B, Elder K. 2000. Combining binary decision tree and geostatistical methods to estimate snow distribution in a mountain watershed. *Water Resources Research* **36**(1): 13–26.

Bales RC, Molotch NP, Painter TH, Dettinger MD, Rice R, Dozier J. 2006. Mountain hydrology of the western United States. *Water Resources Research* **42**: WO8432, doi.10.1029/2005WR004387.

Barnett TP, Adam JC, Lettenmaier DP. 2005. Potential impacts of a warming climate on water availability in snow-dominated regions. *Nature* **438**(7066): 303–309.

Barry R, Prevost M, Stein J, Plamondon AP. 1990. Application of a snow cover energy and mass balance model in a balsam fir forest. *Water Resources Research* **26**(5): 1079–1092.

Berbigier P, Bonnefond JM. 1995. Measurement and modeling of radiation transmission within a stand of maritime pine (Pinus-Pinaster Ait). *Annales Des Sciences Forestieres* **52**(1): 23–42.

Bosch JM, Hewlett JD. 1982. A review of catchment experiments to determine the effect of vegetation changes on water yield and evapotranspiration. *Journal of Hydrology* **55**(1–4): 3–23.

Breiman L, Friedman J, Stone CJ, Olshen RA. 1984. *Classification and Regression Trees*. Chapman & Hall/CRC: Boca Raton, FL; 368.

Breshears DD, Cobb NS, Rich PM, Price KP, Allen CD, Balice RG, Romme WH, Kastens JH, Floyd ML, Belnap J, Anderson JJ, Meyers OB, Meyers CW. 2005. Regional vegetation die-off in response to global-change-type drought. *Proceedings of the National Academy of Sciences of the United States of America* **102**(42): 15144–15148.

Clark LA, Pregibon D. 1992. Tree-based models. In *Statistical Models*, Chambers JM, Hastie TJ (eds): S. Wadsworth & Brooks; Pacific Grove, CA; 608.

Cline D, Armstrong R, Davis R, Elder K, Liston G. 2001. NASA Cold Land Processes Field Experiment Plan 2001–2004. NASA Earth Science Enterprise, Land Surface Hydrology Program.

Cline D, Armstrong R, Davis R, Elder K, Liston G. 2002. updated 2003. *CLPX-Ground: ISA Snow Depth Transects and Related Measurements*, In situ data edited by Parsons M, Brodzik MJ (eds). National Snow and Ice Data Center: Boulder, CO.

Day RJ. 1972. Stand structure, succession, and use of southern albertas rocky mountain forest. *Ecology* **53**(3): 472–478.

Elder K, Rosenthal W, Davis RE. 1998. Estimating the spatial distribution of snow water equivalence in a montane watershed. *Hydrological Processes* **12**(10–11): 1793–1808.

Erickson TA, Williams MW, Winstral A. 2005. Persistence of topographic controls on the spatial distribution of snow in rugged mountain terrain, Colorado, United States. *Water Resources Research* **41**: W04014.

Erxleben J, Elder K, Davis R. 2002. Comparison of spatial interpolation methods for estimating snow distribution in the Colorado Rocky Mountains. *Hydrological Processes* **16**(18): 3627–3649.

Essery R, Pomeroy J, Parviainen J, Storck P. 2003. Sublimation of snow from coniferous forests in a climate model. *Journal of Climate* **16**(11): 1855–1864.

Ffolliott PF, Gottfried GJ, Baker MB. 1989. Water yield from forest snowpack management—Research findings in Arizona and New-Mexico. *Water Resources Research* **25**(9): 1999–2007.

Fu P, Rich PM. 2000. *The Solar Analyst 1·0 Manual*. Helios Environmental Modeling Institute (HEMI): Lawrence, KS.

Geddes CIA, Brown DG, Fagre DB. 2005. Topography and vegetation as predictors of snow water equivalent across the alpine treeline ecotone at Lee Ridge, Glacier National Park, Montana, USA. *Arctic Antarctic and Alpine Research* **37**(2): 197–205.

Gelfan AN, Pomeroy JW, Kuchment LS. 2004. Modeling forest cover influences on snow accumulation, sublimation, and melt. *Journal of Hydrometeorology* **5**(5): 785–803.

Goff F, Gardner JN, Reneau SL, Goff CJ. 2006. Preliminary geologic map of the Valles San Antonio quadrangle, Sandoval County, New Mexico. New Mexico Bureau of Geology and Mineral Resources. Open-file Geologic Map OF-GM 132, scale 1 : 24000.

Golding DL, Swanson RH. 1978. Snow accumulation and melt in small forest openings in Alberta. *Canadian Journal of Forest Research-Revue Canadienne De Recherche Forestiere* **8**(4): 380–388.

Golding DL, Swanson RH. 1986. Snow distribution patterns in clearings and adjacent forest. *Water Resources Research* **22**(13): 1931–1940.

Goodison BE, Louie PYT, Yang D. 1998. *WMO Solid Precipitation Measurement Intercomparison Final Report*. World Meteorological Organization: Geneva.

Gustafson JR, Brooks PD, Veatch WC, Broxton PD. in review. Quantifying Variations in Snow Water Equivalent, Chemistry, and Water Isotopes in a Montane Snowpack.

Harding RJ, Pomeroy JW. 1996. Energy balance of the winter boreal landscape. *Journal of Climate* **9**(11): 2778–2787.

Hardy JP, Davis RE, Jordan R, Li X,Woodcock C, Ni W, Mckenzie JC. 1997. Snow ablation modeling at the stand scale in a boreal jack pine forest. *Journal of Geophysical Research-Atmospheres* **102**(D24): 29397–29405.

Hardy JP, Melloh R, Koenig A, Marks D, Winstral A, Pomeroy JW, Link T. 2004. Solar radiation transmission through conifer canopies. *Agricultural and Forest Meteorology* **126**: 257–270.

Hedstrom NR, Pomeroy JW. 1998. Measurements and modelling of snow interception in the boreal forest. *Hydrological Processes* **12**(10–11): 1611–1625.

Hiemstra CA, Liston GE, Reiners WA. 2002. Snow redistribution by wind and interactions with vegetation at upper treeline in the Medicine Bow Mountains, Wyoming, USA. *Arctic Antarctic and Alpine Research* **34**(3): 262–273.

Hornbeck JW, Martin CW, Eagar C. 1997. Summary of water yield experiments at Hubbard Brook Experimental Forest, New Hampshire. *Canadian Journal of Forest Research-Revue Canadienne De Recherche Forestiere* **27**(12): 2043–2052.

Iverson LR, Prasad AM. 1998. Predicting abundance of 80 tree species following climate change in the eastern United States. *Ecological Monographs* **68**(4): 465–485.

Li XW, Strahler AH, Woodcock CE. 1995. A hybrid geometric optical-radiative transfer approach for modeling albedo and directional reflectance of discontinuous canopies. *IEEE Transactions on Geoscience and Remote Sensing* **33**(2): 466–480.

Liston GE, Elder K. 2006. A distributed snow-evolution modeling system (SnowModel). *Journal of Hydrometeorology* **7**(6): 1259–1276.

McClung D, Schaerer P. 2000. *The Avalanche Handbook*. The Mountaineers: Seattle, WA; 271.

McDowell N, White SA, Pockman W. 2008. Transpiration and stomatal conductance across a steep climate gradient in the southern Rocky Mountains. *Ecohydrology* **1**: 193–204.

McKay GA, Gray DM. 1981. The distribution of snowcover. In *The Handbook of Snow*, Gray DM, Male DH (eds). Pergamon Press: New York.

Molotch NP, Colee MT, Bales RC, Dozier J. 2005. Estimating the spatial distribution of snow water equivalent in an alpine basin using binary regression tree models: the impact of digital elevation data and independent variable selection. *Hydrological Processes* **19**(7): 1459–1479.

Molotch NP, Blanken PD, Williams MW, Turnipseed AA, Monson RK, Margulis SA. 2007. Estimating sublimation of intercepted and subcanopy snow using eddy covariance systems. *Hydrological Processes* **21**(12): 1567–1575.

Musselman KN. 2006. *Quantifying the effects of forest vegetation on snow accumulation, ablation, and potential meltwater inputs, Valles Caldera National Preserve, NM, USA*. Master's Thesis, University of Arizona, Tucson.

Musselman KN, Molotch NP, Brooks PD. 2008. Effects of vegetation on snow accumulation and ablation in a mid-latitude sub-alpine forest. *Hydrological Processes* **22**: 2767–2776.

National Research Council. 2007. *Earth Science and Applications from Space: National Imperatives for the Next Decade and Beyond*. National Academies Press: Washington, DC.

Pierce LL, Running SW. 1988. Rapid estimation of coniferous forest Leaf-area index using a portable integrating radiometer. *Ecology* **69**(6): 1762–1767.

Pomeroy JW, Gray DM, Hedstrom NR, Janowicz JR. 2002. Prediction of seasonal snow accumulation in cold climate forests. *Hydrological Processes* **16**(18): 3543–3558.

Pomeroy JW, Gray DM, Shook KR, Toth B, Essery RLH, Pietroniro A, Hedstrom N. 1998a. An evaluation of snow accumulation and ablation

processes for land surface modelling. *Hydrological Processes* **12**(15): 2339–2367.

Pomeroy JW, Parviainen J, Hedstrom N, Gray DM. 1998b. Coupled modelling of forest snow interception and sublimation. *Hydrological Processes* **12**(15): 2317–2337.

Rinehart AJ, Vivoni ER, Brooks PD. 2008. Effects of vegetation, albedo, and radiation sheltering on the distribution of snow in the Valles Caldera, New Mexico. *Ecohydrology* **1**: 253–270.

Tolt G. 2003. *Determining Edgeness Using Homogeneity of Templates, Procedings of the 12th IEEE International Conference on Fuzzy Systems, 2003*. Institute of Electrical and Electronics Engineers: St. Louis, MO.

United States Geological Survey. 2003. *Valles Caldera National Preserve 10m Digital Elevation Model*. University of New Mexico Earth Data Analysis Center: Albuquerque, NM.

United States Geological Survey. 2007. *NLCD 2001 Land Cover*. United States Geological Survey: Sioux Falls, SD.

United States Geological Survey. 2008. *Elevation, National Elevation Database*. United States Geological Survey, Eros Data Center: Sioux Falls, SD.

Wang YP. 2003. A comparison of three different canopy radiation models commonly used in plant modelling. *Functional Plant Biology* **30**(2): 143–152.

Webb T, Bartlein PJ. 1992. Global changes during the last 3 Million Years—Climatic controls and biotic responses. *Annual Review of Ecology and Systematics* **23**: 141–173.

Westerling AL, Hidalgo HG, Cayan DR, Swetnam TW. 2006. Warming and earlier spring increase western US forest wildfire activity. *Science* **313**(5789): 940–943.

Wigmosta MS, Vail LW, Lettenmaier DP. 1994. A distributed Hydrology-vegetation model for complex terrain. *Water Resources Research* **30**(6): 1665–1679.

Winstral A, Elder K, Davis RE. 2002. Spatial snow modeling of wind-redistributed snow using terrain-based parameters. *Journal of Hydrometeorology* **3**(5): 524–538.

Yamazaki T, Kondo J. 1992. The snowmelt and heat-balance in snow-covered forested areas. *Journal of Applied Meteorology* **31**(11): 1322–1327.

Zhang YS, Suzuki K, Kadota T, Ohata T. 2004. Sublimation from snow surface in southern mountain taiga of eastern Siberia. *Journal of Geophysical Research* **109**: D21103.

DOI: 10.1002/eco